Optical measurement of the isotope shifts and hyperfine and superhyperfine interactions of Nd in the solid state

R. M. Macfarlane
IBM Research Division, Almaden Research Center, 650 Harry Road, San Jose, California 95120-6099

R. S. Meltzer
Department of Physics and Astronomy, The University of Georgia, Athens, Georgia 30602

B. Z. Malkin
Physics Department, Kazan State University, Kazan 420008, Russian Federation

(Received 24 March 1998)

We report the observation of optically resolved isotope, hyperfine, and superhyperfine structure in the spectrum of Nd^{3+} ions in $YLiF_4$, isotopically pure in ^7Li. This observation was made on the $(4f^3-4f^3)$, $^4I_{9/2}(1)\rightarrow{}^4F_{3/2}(1)$ transition of Nd^{3+} ions present as impurities at ppm levels. The optical linewidths of the transitions of the even mass number isotopes, ^{142}Nd, ^{144}Nd, ^{146}Nd, ^{148}Nd, and ^{150}Nd, are only 45 MHz which makes it very easy to resolve the isotope shift of 115 MHz/unit mass. The hyperfine structure of the two odd mass number isotopes, ^{143}Nd and ^{145}Nd, are resolved and the hyperfine parameters are determined in both the ground and electronically excited states. Some of the transitions have linewidths as narrow as 10 MHz. These are the narrowest optical inhomogeneous linewidths observed in solids. In addition, each even isotope line is split by 30 MHz. The observed splitting is assigned to a superhyperfine coupling between Nd^{3+} and its nearest-neighbor fluorine nuclei. Here, a superhyperfine splitting has been resolved in an optical spectrum. The optical line shapes for the even isotopes are calculated as the sum of all transitions between the superhyperfine components (Nd^{3+} with its eight nearest-neighbor F nuclei) of the ground and excited electronic states, considering both magnetic dipole-dipole (including spin-transfer contributions) and contact interactions. The results are in quantitative agreement with experiment. [S0163-1829(98)07333-0]

I. INTRODUCTION

We recently showed[1] that because of remarkably small crystal strain contributions, the inhomogeneous broadening of the optical transitions of Er^{3+} ions in $YLiF_4$, isotopically pure in ^7Li, was limited by a qualitatively new mechanism—the local spin fields due to the fluorine nuclei in the $YLiF_4$ lattice acting on the Er^{3+} electronic states. Here we report that this is also true of the inhomogeneous linewidth of the $^4I_{9/2}(1)\rightarrow{}^4F_{3/2}(1)$ optical transition of Nd^{3+} ions in Y^7LiF_4 and that, in this case, coupling to the F spin gives rise to additional structure. Optical absorption lines corresponding to the even mass number isotopes ^{142}Nd, ^{144}Nd, ^{146}Nd, ^{148}Nd, and ^{150}Nd are clearly resolved, as is hyperfine structure of the two odd mass number isotopes: ^{143}Nd, ^{145}Nd. In addition it is possible to resolve a very small (30 MHz) splitting which is assigned to the superhyperfine interaction between the Nd electronic levels and the nuclear-spin moments on the neighboring fluorine ions. Here, a superhyperfine splitting has been resolved in an optical spectrum.

There is a very large body of work on isotope shifts of Nd(I) and Nd(II) in atomic spectroscopy.[2] These involve parity-allowed transitions between different electronic configurations. Typical isotope shifts are 0.1–1 GHz/unit mass and arise from the different electron density at the nuclei whose volume is mass dependent as well as from a pure mass effect. Since we are dealing here with transitions within the f shell, such effects are negligible, and isotope shifts are instead attributed to local lattice deformation[3] and differential coupling to zero-point phonons whose frequencies are mass dependent.[1,4] Pelletier-Allard and Pelletier[5] measured the isotope shifts of Nd ions in $LaCl_3$ by selective enrichment and the measurement of corresponding resonances for the different isotopes in separate crystals. The linewidths of ~4 GHz were considerably larger than the isotope shifts (~180 MHz/unit mass) introducing some uncertainty in the measurement. The present measurements were made on a single sample with the natural abundance of the isotopes and an inhomogeneous linewidth much less than the isotope shift.

While superhyperfine structure in the electron paramagnetic resonance spectra of rare-earth ions is well known (e.g., Yb^{3+} in CaF_2),[6] this is an observation in the optical spectrum. The observation is made possible by the unusually small crystal strain broadening of the optical transitions. The calculation of the superhyperfine structure presented here considers not only the magnetic dipole-dipole (MDD) interaction between the Nd^{3+} electron and F nuclear spins but also the spin transfer and contact interactions. This type of calculation is similar to that used to explain, for example, electron nuclear double-resonance spectra of rare-earth ions such as divalent europium[7] and thulium.[8] The calculation provides support to the assignment of the splitting to superhyperfine interactions and also allows one to estimate the relative contributions of the MDD and of the contact and spin-transfer interactions.

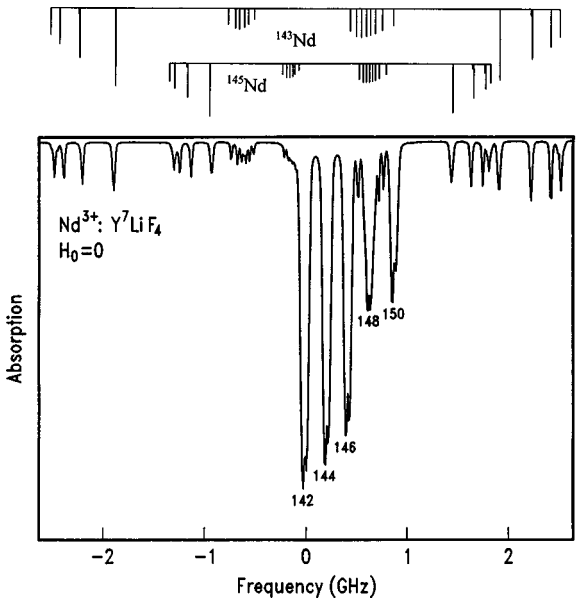

FIG. 1. Fluorescence excitation spectrum of Nd isotopes in Y^7LiF_4 at 1.6 K. Isotopic mass numbers are shown. Hyperfine structure for the two odd isotopes are compared with those calculated for the Hamiltonian [Eq. (1)] using the parameters in Table I.

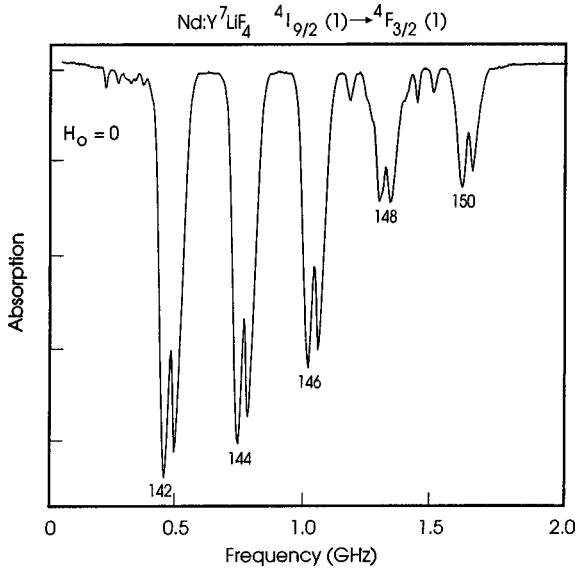

FIG. 2. Expanded view of the even isotope spectrum at 1.6 K showing the splitting due to the superhyperfine interactions with the neighboring fluorine nuclei.

II. EXPERIMENTAL RESULTS

Experiments were carried out using the same crystal of Y^7LiF_4 containing 99.9% pure ^{7}Li which was used in our previous work.[1] Isotopic purification of lithium was found to be necessary in order to remove the contribution to the inhomogeneous broadening due to the random distribution of ^{6}Li and ^{7}Li in the lattice.[9] Neodymium was present as an unintentional trace impurity with a concentration estimated to be several ppm. The trivalent neodymium ions substitute for yttrium ions in sites of S_4 symmetry. Absorption on the $^4I_{9/2}(1)\rightarrow{}^4F_{3/2}(1)$ transition at 11535.7 cm^{-1} is σ polarized and was measured at 1.6 K in an excitation spectrum monitoring the emission around 1.05μ by scanning a single frequency Ti:sapphire laser whose linewidth was $\sim$1 MHz. The resulting spectrum is shown in Fig. 1. EPR measurements[10] and g-value calculations[11] show that the ground state belongs to the $\Gamma_{7,8}$ representation of S_4, and since the optical transition is σ polarized, selection rules require that the excited state also has $\Gamma_{7,8}$ symmetry. In addition to their differential isotope shifts, each even isotope line shows an additional splitting of 30 MHz as shown more clearly in the higher resolution spectrum of Fig. 2. The identical line shape of each even isotope transition shows an asymmetry with the low-frequency component more intense. The relative intensities of the lines correspond well with the percentage natural abundance: 27.1% ^{142}Nd, 23.9% ^{144}Nd, 17.8% ^{146}Nd, 5.7% ^{148}Nd, and 5.6% ^{150}Nd. The correspondence is not exact because of the forest of odd isotope hyperfine lines (28 at zero magnetic field, 56 in a field), some of which overlap the even isotope transitions. In Fig. 3 the spectrum in an applied dc magnetic field of $H=440$ G, along the crystal c axis, is shown. Each of the even isotope lines is split by the field into two lines whose widths are remarkably narrow (45 MHz) enabling an accurate measurement of the isotope shift as 115 MHz/unit mass. The narrower linewidths and the larger isotope shifts than in the corresponding erbium spectrum makes this the most clearly resolved example of isotope structure yet observed in the solid state. It should be pointed out that such narrow lines will only be observed for very low doping levels.

The remaining lines in Figs. 1–3, in addition to those due to the even isotopes, arise from transitions between the hyperfine components of the ground and excited states for the two odd isotopes (12.2% ^{143}Nd, 8.3% ^{145}Nd). Both have nuclear spins of 7/2 and exhibit hyperfine splittings totaling several GHz. Because of the presence of two odd isotopes, the hyperfine spectrum is considerably more complicated than in the case of ^{167}Er. Assignment of a particular transition to ^{143}Nd or ^{145}Nd is indicated by the bar graphs above the spectrum in Fig. 1 and is based on a calculation described below. In the applied field, it is seen from Fig. 3 that some of the hyperfine transitions of the odd isotopes are even narrower than those of the even isotope lines with some linewidths as small as 10 MHz.

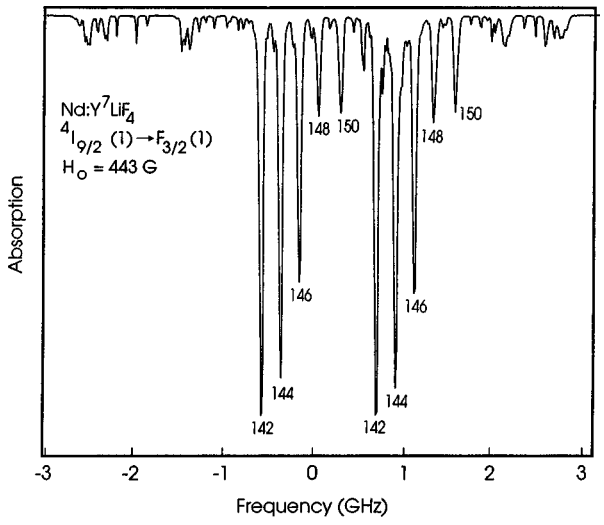

FIG. 3. Optical Zeeman effect for the Nd isotopes in Y^7LiF_4 at 1.6 K for an external field $\mathbf{H}_0 \| c$.

TABLE I. Hyperfine parameters for Nd^{3+}:$YLiF_4$.

	$^4I_{9/2}(1)$ (expt. from Ref. 7)	$^4I_{9/2}(1)$ (Calc.)	$^4F_{3/2}(1)$ (expt.)	$^4F_{3/2}(1)$ (Calc.)
$A(143)$, $B(143)$ MHz	−590, −789	−521, −820	−252, −479	−273, −449
$A(145)$, $B(145)$ MHz	−372, −497	−324, −510	−159, −302	−170, −279
$A(143)/A(145)$	1.59	1.61	1.59	1.61
$B(143)/B(145)$	1.59	1.61	1.59	1.61
$\mu_N(143)/\mu_N(145)$	1.64	1.64	1.64	1.64
$g_\parallel$	1.987	1.733	<0.1	0.104
$g_\perp$	2.554	2.730	0.80	0.903

III. THEORETICAL ANALYSIS AND DISCUSSION

A. Hyperfine splittings of odd nuclear spin isotopes

The hyperfine spectra of the ^{143}Nd and ^{145}Nd isotopes are analyzed as was done previously for ^{167}Er in $YLiF_4$.[1] The spin Hamiltonian for the ground and excited states is

$$\mathcal{H}=g_\parallel\beta H_z S_z+g_\perp\beta(H_xS_x+H_yS_y)+AI_zS_z+B(I_xS_x+I_yS_y)+P[I_z^2-I(I+1)/3], \quad (1)$$

where $g_\parallel$ and $g_\perp$ are the components of the g factor parallel and perpendicular to the c axis, H_α are the components of the external magnetic field, and S and I are the electron- and nuclear-spin operators, respectively. A and B are the hyperfine parameters, and P is the quadrupole constant. The hyperfine matrices for ^{167}Er, ^{143}Nd, and ^{145}Nd are all identical since all three isotopes have a nuclear spin of $I=7/2$ and an electron spin $S=1/2$.

The ground-state hyperfine parameters for both odd Nd isotopes are well known.[11] The excited-state parameters were varied to give a best fit to the spectrum. The eigenvalue results are shown by the positions of the sticks in the graphs above the spectrum in Fig. 1 and provide an excellent fit to the observed transition frequencies. The heights of the sticks indicate the predicted relative transition probabilities and include the relative isotopic abundance ratios of the two Nd isotopes. The stick heights should be compared with the integrated area of the observed lines since their widths are unequal. The agreement is quite good. The resulting hyperfine parameters are summarized in Table I along with the observed g values. The quadrupole constant is found to be small and a value of zero for these two electronic states provides an excellent description of the observed spectrum.

Some of the hyperfine lines of ^{143}Nd and ^{145}Nd exhibit even narrower linewidths than those of the even isotopes as can be seen from Figs. 1 and 3. An understanding of the broadening of individual hyperfine components is complicated by the fact that the magnetic moments of the different hyperfine levels are unequal and some of them are nonmagnetic singlets derived from the integer ($F=3,4$) angular momentum of the coupled electron/nuclear spin system. This was also found for the case of ^{167}Er. However, for the $\Gamma_{7,8}\rightarrow\Gamma_{7,8}$ transition studied here (σ polarization), singlet-singlet transitions are forbidden. The line shapes of each of the hyperfine transitions can be calculated by solving the combined hyperfine and superhyperfine Hamiltonians in the ground and excited state and summing over all transitions. However, an estimate for the linewidths can be obtained by calculating the magnetic moment differences for the ground and excited states involved in each transition and taking the products of this with the local fluorine spin fields. The fluorine spin field, whose magnitude is estimated below, amounts to about 5–10 G. For most of the transitions, the magnetic moment differences fall in the range of 0.5–1.5 MHz/G indicating that the superhyperfine contributions to the linewidths should fall within the range 2.5–15 MHz. We therefore conclude that the combined effect of homogeneous and strain-induced inhomogeneous contributions to the linewidths are about 10 MHz and the remainder of the linewidth, variable from transition to transition, results from superhyperfine interactions. To our knowledge, these are the narrowest inhomogeneously broadened optical absorption lines observed in the solid state.

B. Superhyperfine spectrum of even mass number isotopes

The observation of a splitting of each even isotope line is new and is assigned to the superhyperfine coupling between the Nd^{3+} electronic levels and the nuclear moments of the neighboring fluorines. There is no analog in the case of atomic spectroscopy. This interaction causes a doublet shape of the optical transition which results from the removal of the Kramers' degeneracy of the Nd^{3+} electronic levels. The splitting is described as a pseudosplitting which results from the specific distribution of the electron-nuclear states of the Nd^{3+} ion and its eight nearest-neighbor ligand nuclei. Superhyperfine interactions with F nuclei outside this first coordination sphere contribute to the observed linewidths through both homogeneous and inhomogeneous line broadening but that they are too small to produce any resolvable splitting. At the ppm Nd^{3+} concentration of this sample, Nd-Nd interactions do not make a significant contribution to the line shapes.

A model which can be used to interpret the broadening resulting from F nuclei outside the first coordination sphere is one in which the magnetic moment of Nd^{3+} ion produces a ''frozen core'' [12] of fluorine nuclei whose ability to mutually spin flip with their neighbors is reduced by their detuning in the field of the paramagnetic ion. These Nd-F interactions produce both a homogeneous and inhomogeneous contribution to the linewidth. With increasing distance from the Nd^{3+} ion, the fluorine spin-flip rate increases so that more distant fluorine nuclei outside the frozen core produce a small random fluctuating component of the local magnetic field which makes a major contribution to the homogeneous

broadening. The random distribution of spin orientations within the frozen core contribute to the inhomogeneous broadening. Separation of the homogeneous and inhomogeneous contributions is difficult since it depends on the time scale of the experiment. The observation of strongly nonexponential photon echo decay[13] and time-dependent spectral hole burning[14] for another Kramers ion, Er^{3+} in $YLiF_4$, indicates the presence of strong spectral diffusion. For the purpose of this discussion, the separation is not important and the contribution to the linewidth from F nuclear spins outside the first coordination sphere is treated as a parameter in the calculations of the superhyperfine splitting.

Inside the frozen core, this largely static local field, along with crystal strains and inhomogenieties, determines the inhomogeneous transition lineshapes. The expected magnitude of the contribution of the superhyperfine interactions to the linewidth and pseudo-splitting is calculated later in this section but an estimate is easily obtained as follows. The frequency shift due to the magnetic dipole-dipole (MDD) interaction between the Nd^{3+} electron-spin moment and the surrounding fluorine nuclear moments is obtained from $H_{\rm loc}$, the local magnetic field acting at the Nd^{3+} site, and is given by

$$\Delta\nu = \pm 1/2(g \pm g')\beta H_{\rm loc} \tag{2}$$

for the four Zeeman transitions where the g values for the ground state and excited states (see Table I) were obtained from EPR (Ref. 11) and our optical measurements, respectively. The value of $H_{\rm loc}$ at the Nd nucleus due to a single nearest-neighbor F nucleus at a distance of 2.23 Å is about 1–2 G, depending on the relative orientations of the electron and nuclear spins with respect to the direction of the line connecting them. The total local field from the eight nearest neighbors will then typically be 5–10 G since in general they will not be aligned. This yields expected frequency shifts of about 7–14 MHz which is of the same size as half of the observed splittings. (The splitting is twice the shift of each transition.) However, because of the random distribution of F nuclear spin moments, one might expect just an inhomogeneous broadening, not a splitting at zero field.

To address this problem, full diagonalizations of the superhyperfine interaction in the ground and excited electron-spin states were performed including MDD coupling, transferred spin density, and contact terms for the Nd electron spin coupled to the eight nearest F nuclear spins. The contributions from all transitions between these electron-nuclear states were summed to obtain the full line shape.

The nearest surroundings of the impurity Nd^{3+} ion, substituting for a Y^{3+} ion, contains two groups of four F^- ions, each group mutually transforming among themselves under the S_4 symmetry operations. In the crystallographic coordinate system with the origin at the Nd(Y) site, the coordinates of two inequivalent F^- ions, in particular, F_1 and F_5, are equal to $x_1=(0.5-x)a$; $y_1=(0.5-y)a$; $z_1=zc$; $x_5=(0.5-x)a$; $y_5=-ya$; $z_5=(0.25-z)c$; where $x=0.2821$, $y=0.1642$, $z=0.0815$, and the lattice constants are $a=5.168$ Å, $c=10.731$ Å.[15] The coordinates of the other six ligand nuclei are easily obtained with the operations C_2 and S_4. The contribution due to the superhyperfine interaction is included by adding to the spin Hamiltonian (1)

$$\mathcal{H}_{\rm shf} = \Sigma_{i\alpha\beta} I_{i,\alpha} a_{\alpha\beta}(i) S_\beta, \tag{3}$$

where the summation is over eight F nuclei with the spin moments $\mathbf{I}_i$ ($i=1$ to 8), and the coupling constants can be expressed as

$$a_{\alpha\beta}(i) = a_{\alpha\beta,d}(i) + a_{\alpha\beta,s}(i) + a_{\alpha\beta,p}(i). \tag{4}$$

The first, second, and third terms in Eq. (4) correspond, respectively, to the MDD interaction, and the spin transfer from the Nd^{3+} ion onto the $2s$ and $2p$ ligand orbitals. It should be noted that, for S_4 symmetry, when using the crystallographic system of coordinates,[16] the $g_\perp$ factor in the spin Hamiltonian (1) is to be replaced by $g_\perp \cos\varphi$, and the term $\beta g_\perp \sin\varphi(H_y S_x - H_x S_y)$ is to be added, with the corresponding changes in the hyperfine terms. The angle φ is determined by the wave functions $|+\rangle$, $|-\rangle$ of the electronic doublet:

$$g_\perp \cos\varphi = 2g_J \mathrm{Re}\langle + |J_x| - \rangle,$$

$$g_\perp \sin\varphi = 2g_J \mathrm{Im}\langle + |J_x| - \rangle, \tag{5}$$

(g_J is the Lande factor) and depends on the parameters of the crystal-field Hamiltonian ($\mathcal{H}_{\rm cf} = \Sigma B_p^k O_p^k$, where O_p^k are the Stevens operators). Explicit expressions for the point magnetic dipole contributions $a_{\alpha\beta,d}$ are given in the Appendix.

For the numerical evaluations, we have used the crystal-field parameters[16] transformed to the crystallographic system of coordinates according to Ref. 17:

$$B_2^0 = 212;\quad B_4^0 = -118;\quad B_4^4 = -945;\quad B_4^{-4} = -818;$$

$$B_6^0 = -1.5;\quad B_6^4 = -570;\quad B_6^{-4} = -493\ \mathrm{cm}^{-1}.$$

Neglecting J-mixing effects, we obtained the following wave functions for the ground Kramers' doublet:

$$|\pm\rangle = (-0.4696 \pm 0.4063i)|J_z = \pm 9/2\rangle + 0.6318|J_z = \pm 1/2\rangle + (-0.3508 \mp 0.3035i)|J_z = \mp 7/2\rangle;$$

and $\varphi = -10^{-4}$. Two other sets of crystal-field parameters are available in the literature;[18,19] in all cases $|\varphi|$ does not exceed 0.05.

The energies and wave functions of the excited ^4F states were obtained in the L,S basis by taking into account the crystal-field energy and the spin-orbit interaction. The $J_z = \pm 1/2$ states of the excited doublet $^4F_{3/2}(1)$ are mixed with the corresponding states of the nearest $^4F_{5/2}$ multiplet due to the crystal-field interaction. In particular, for the excited doublet $^4F_{3/2}(1)$ one of the Kramers' conjugate states has the form

$$|+\rangle = 0.9953|^4F_{3/2}, J_z = 1/2\rangle - 0.0627|^4F_{5/2}, J_z = 1/2\rangle - 0.0196|^4F_{7/2}, J_z = 1/2\rangle + (0.0435 + 0.0377i)|^4F_{7/2}, J_z = -7/2\rangle + (0.0306 + 0.0265i)|^4F_{9/2}, J_z = -7/2\rangle.$$

The projections on these crystal-field states of the Zeeman and hyperfine interactions in the free ion, $g_J\beta\mathbf{J}\cdot\mathbf{H} + a_J\mathbf{J}\cdot\mathbf{I}$, produce values of the spin-Hamiltonian parameters (the core

polarization contributions are neglected) which are presented in Table I. Though mixing of the ^4F states with other multiplets due to the spin-orbit interactions is not taken into account, the g factors and the hyperfine parameters are consistent with the experimental data. It is found that a rather small admixture of the $|^4F_J(J>3/2)\rangle$ states produce large changes in $g_\parallel$ which is 0.4 in the case of the pure $|^4F_{3/2}, J_z=\pm 1/2\rangle$.

To obtain explicit expressions for the parameters of the transferred hyperfine interaction, we have used the following procedure. The wave functions of the electronic Kramers doublets are written as linear combinations of the Slater determinants constructed from the one-electron $4f$ spin orbitals. The crystallographic system of coordinates is transformed to the ligand coordinate system with the quantization axis along the ligand radius-vector r_i. The initial $|4fm\rangle$ orbitals are written through the rotational transformation coefficients $D^{(3)}_{m'm}$ and the $|4fm\rangle$ orbitals quantized in the ligand coordinate system. The $|4f0'\rangle$ and $|4f\pm 1'\rangle$ orbitals are replaced with the antibonding molecular orbitals.[20] Finally we return to the crystallographic system of coordinates and substitute the linear combinations of ionic orbitals

$$
\begin{aligned}
|4fm\rangle_{\mathrm{MO}} = |4fm\rangle + \Sigma_i \{ & D^{(3)}_{0m}\lambda_{2s}|2s\rangle_i + [\lambda_{2\sigma}\cos\,\theta_i D^{(3)}_{0m} + \lambda_{2\pi}\sin\,\theta_i (D^{(3)}_{-1m} - D^{(3)}_{1m})/\sqrt{2}]|2p0\rangle_i \\
& - e^{-i\phi}[\lambda_{2\sigma}\sin\,\theta_i D^{(3)}_{0m}/\sqrt{2} + 0.5\lambda_{2\pi}((1+\cos\,\theta_i)D^{(3)}_{1m} + (1-\cos\,\theta_i)D^{(3)}_{-1m})]|2p1\rangle_i \\
& + e^{i\phi}[\lambda_{2\sigma}\sin\,\theta_i D^{(3)}_{0m}/\sqrt{2} - 0.5\lambda_{2\pi}((1-\cos\,\theta_i)D^{(3)}_{1m} + (1+\cos\,\theta_i)D^{(3)}_{-1m})]|2p-1\rangle_i\}; \qquad (6)
\end{aligned}
$$

for the $|4fm\rangle$ functions in the Slater determinants. Here θ_i, ϕ_i are the spherical coordinates of the ligand with the wave functions $|2s\rangle_i$, $|2pm\rangle_i$; λ_{2s}, $\lambda_{2\sigma}$, and $\lambda_{2\pi}$ are the coefficients in the corresponding antibonding molecular orbitals. The explicit expressions for all superhyperfine parameters have been obtained by averaging the hyperfine interaction in the electronic doublets. These expressions are too large to present here, but the simplest two examples are given in the Appendix for the excited state $^4F_{3/2}(1)$ ($|L=3, S=3/2, J=3/2, J_z=\pm 1/2\rangle$).

The parameters of the spin transfer and the contact interaction contain 12 variables, namely the coefficients λ_{2s}, $\lambda_{2\sigma}$, and $\lambda_{2\pi}$ for two groups of inequivalent ligands in the ground and excited electronic states. To diminish the number of variables in the problem, we assumed the following simple relationships between the covalency constants and the corresponding overlap integrals:[21]

$$\lambda_{2s}(i) = k_{2s}S_{2s}(r_i); \quad \lambda_{2\sigma}(i) = k_{2p}S_{2\sigma}(r_i);$$

$$\lambda_{2\pi}(i) = k_{2p}S_{2\pi}(r_i).$$

For the given interionic distances, the overlap integrals S_{2s}, $S_{2\sigma}$, $S_{2\pi}$ have been calculated in Ref. 22, and neglecting the differences between the covalency constants in the ground and excited states, we have only two variables, k_{2s} and k_{2p}. The values of these parameters $k^2_{2s}=0.7$ and $k^2_{2p}=2$ were chosen based on a best fit to the measured line shape, namely the splitting and relative intensities of the two components of the optical transition in zero applied field. It should be noted that the factors k_ψ are to be greater than unity for the antibonding molecular orbitals, but the contradiction between this condition and the k_{2s} value may be only illusory because of the significant reduction of the overlap integrals due to the local lattice expansion around the Nd^{3+} impurity ion. The calculated parameters of the superhyperfine interaction of the Nd^{3+} ion crystal field levels with the two nearest inequivalent ligand nuclei are given in Table II; for other ligands, the corresponding parameters can be easily obtained with the S_4 symmetry operations.

The eigenvalues and eigenvectors of the electron-nuclear excitations in the ground and excited states of the Nd^{3+} ion for the even nuclear isotopes ($I=0$) were obtained with the numerical diagonalization of the matrix corresponding to the operator $\mathcal{H}+\mathcal{H}_{\mathrm{shf}}$. The basis states were chosen as product states of each of the two Nd^{3+} $S=1/2$ electronic states coupled to the nearest-neighbor $I_i=1/2$ fluorine nuclei, generating up to 512 basis states in both the ground and excited states.

In computing the line shapes of the σ-polarized electric dipole transitions between the ground and excited electron-nuclear states we took into account that an effective operator of the electric dipole moment $\mathbf{D}$ has nonzero matrix elements between the ground and excited Kramers' doublets only of the type $|\langle ^4I_{9/2}(1),+|\mathbf{D}|^4F_{3/2}(1),-\rangle| = |\langle ^4I_{9/2}(1),-|\mathbf{D}|^4F_{3/2}(1),+\rangle|$. For each transition we assumed a Gaussian line shape of 7 MHz width which is comparable to the magnetic dipole-dipole interaction of the Nd^{3+} ion with the fluorine nuclei in the next coordination shell.

To illustrate the formation of the specific line shape, we present in Fig. 4 the simulated line shapes of the $^4I_{9/2}(1) - {}^4F_{3/2}(1)$ optical transition, obtained without any fitting parameters, taking into account only the direct MDD contributions to the superhyperfine interaction of the Nd^{3+} ion successively with one ligand nucleus, four equivalent nuclei, and all eight nearest-neighbor fluorine nuclei. The spectral envelopes have been computed as the sums of all 4^2, 32^2, and 512^2 possible transitions, respectively. For all cases considered, at zero magnetic field an asymmetric doublet is calculated with the larger intensity at lower frequency, in agreement with experiment (Fig. 2). The widths of the doublet components and the splitting increase with the number of ligand nuclei, and a maximum splitting of 22 MHz is calculated, which is about 73% of what is observed. An improved fit to the splitting is obtained by including spin transfer and contact terms described above. The line shapes, calculated

TABLE II. Tensors of the ligand hyperfine interaction (MHz). Contact $[a_{\alpha\beta,s}(i)]$ and spin transfer $[a_{\alpha\beta,p}(i)]$ terms are in units of k_{2s}^2 and k_{2p}^2, respectively.

	$^4F_{3/2}$						
α	β	$a_{\alpha\beta,d}(1)$	$a_{\alpha\beta,s}(1)$	$a_{\alpha\beta,p}(1)$	$a_{\alpha\beta,d}(5)$	$a_{\alpha\beta,s}(5)$	$a_{\alpha\beta,p}(5)$
x	x	−0.7257	−2.7279	0.2856	−0.7668	−2.3266	0.0095
x	y	3.4305	−0.4695	−0.0185	−1.5126	0.4305	0.0069
y	x	3.4305	−0.4695	−0.0185	−1.5126	0.4305	0.0069
x	z	0.1921	0.0325	0.2804	0.3581	−0.4709	0.7036
z	x	1.7288	0.0325	0.0124	3.2231	−0.4709	−0.0508
y	y	2.3348	−3.1468	0.2691	−1.6343	−2.0797	0.0134
y	z	0.2960	0.0502	0.4321	−0.2699	0.3548	−0.5302
z	y	2.6642	0.0502	0.0192	−2.4288	0.3548	0.0383
z	z	−0.1788	−1.2697	−1.0883	0.2668	−1.0258	−0.6430
	$^4I_{9/2}$						
α	β	$a_{\alpha\beta,d}(1)$	$a_{\alpha\beta,s}(1)$	$a_{\alpha\beta,p}(1)$	$a_{\alpha\beta,d}(5)$	$a_{\alpha\beta,s}(5)$	$a_{\alpha\beta,p}(5)$
x	x	−2.0595	−2.4900	−0.0878	−2.1761	−0.9394	−0.3232
x	y	9.7349	0.4536	0.4125	−4.2925	−0.3689	−0.2709
y	x	9.7349	0.5056	0.4497	−4.2925	−0.4206	−0.2755
x	z	3.8168	−0.3789	0.2710	7.1160	−0.3189	0.4337
z	x	4.9060	0.6731	0.3779	9.1446	0.4096	0.6318
y	y	6.6257	−2.0254	0.3621	−4.6378	−1.1051	−0.4478
y	z	5.8820	−0.8588	0.4571	−5.3623	0.3216	−0.3447
z	y	7.5605	1.2030	0.5848	−6.8924	−0.2830	−0.4745
z	z	−3.5525	−0.6382	−0.5986	5.3012	−1.6500	−0.1940

with the final set of superhyperfine parameters, as a function of magnetic field along the c axis are shown in Fig. 5. The ratio of intensity of the low-frequency and high-frequency doublet components in zero field is somewhat greater than that seen in the measured spectrum. The calculated splitting as a function of field is compared with experiment in Fig. 6. The splitting is nonlinear at low fields and the magnetic-field dependence agrees well with experiment.

The relative importance of the superhyperfine interactions in the ground and excited states are presented in Fig. 7 which shows the calculated density of states for both states. It is clear that the superhyperfine splittings in the ground state are dominant in determining the observed line shapes.

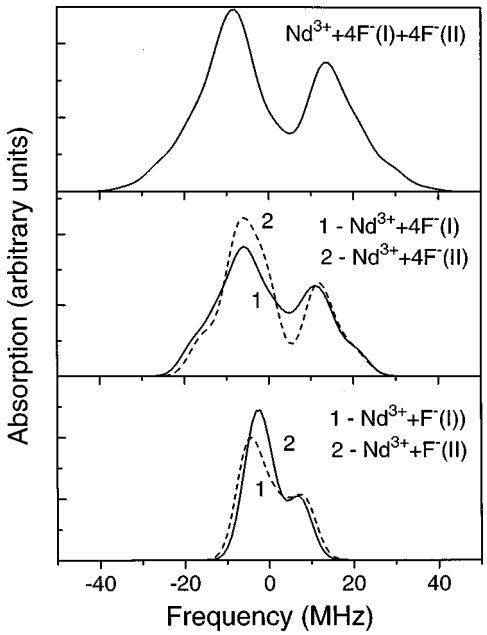

FIG. 4. Spectral envelopes of the $\Gamma_{7,8}(^4I_{9/2}) \Rightarrow \Gamma_{7,8}(^4F_{3/2})$ transition for magnetic dipole-dipole interactions between the fluorine nuclei and the magnetic moment of the Nd^{3+} ion.

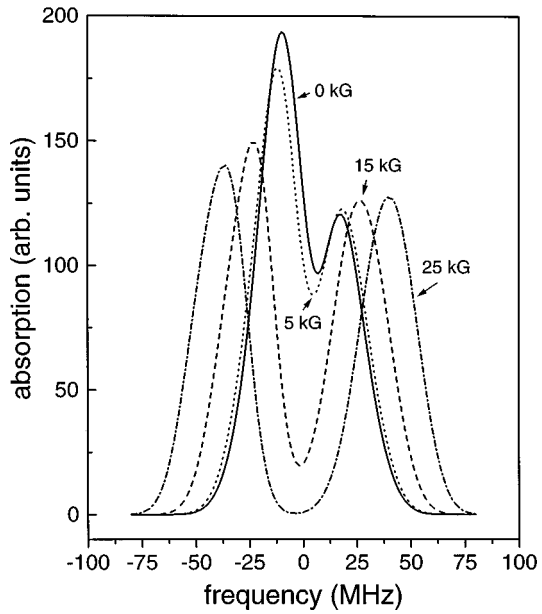

FIG. 5. The simulated line shapes of the $\Gamma_{7,8}(^4I_{9/2}) \Rightarrow \Gamma_{7,8}(^4F_{3/2})$ transition including MDD, transferred spin, and contact interactions in an applied magnetic field $\mathbf{H}_0 \| c$: $H_0 = 0$, 5, 15, and 25 G.

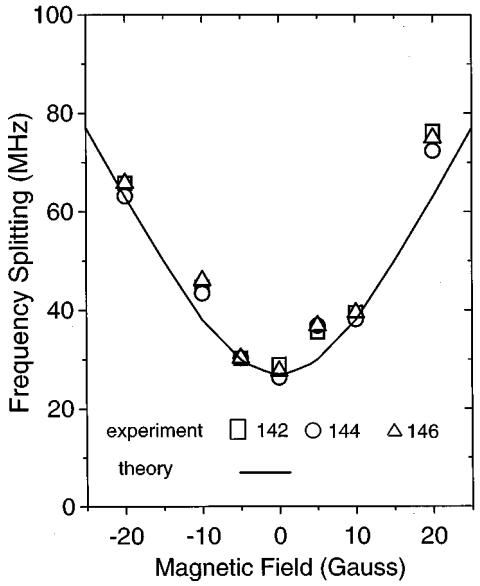

FIG. 6. The magnetic-field dependence of the splitting of the $\Gamma_{7,8}(^4I_{9/2}) \Rightarrow \Gamma_{7,8}(^4F_{3/2})$ transition (solid line indicates theory, open symbols indicate the experiment).

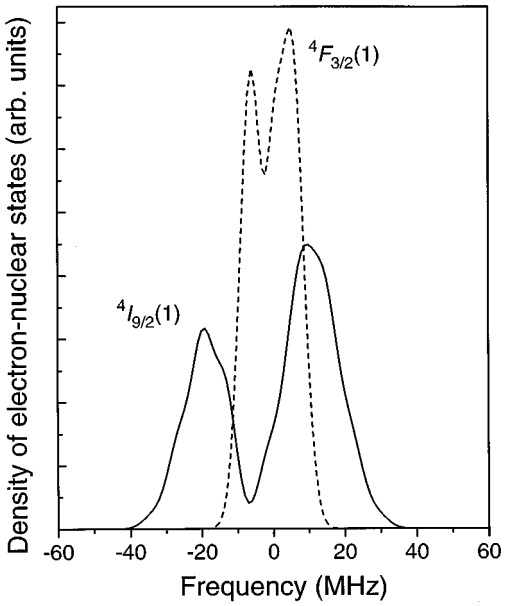

FIG. 7. Density of electron-nuclear states in the Nd^{3+} ion ground state (1) and in the lower sublevel of the $^4F_{3/2}$ multiplet (2).

IV. CONCLUSION

Highly resolved structure with linewidths as small as 10 MHz is observed in the optical spectrum of Nd^{3+} in Y^7LiF_4. The structure in the line shape of the $^4I_{9/2}(1) \rightarrow {}^4F_{3/2}(1)$ transition is explained in terms of an isotope shift and superhyperfine interactions for the even mass number isotopes with the addition of hyperfine effects for the odd isotopes. The hyperfine parameters of the $^4F_{3/2}(1)$ excited state are obtained for both odd isotopes. The doublet structure for the even isotopes in zero magnetic field, observed for the first time, is ascribed to the superhyperfine interaction of the Nd^{3+} Kramers doublet electron-spin states with the eight fluorine ligand nuclear spins. The line shape is calculated by solving for the eigenvalues and eigenvectors of the superhyperfine Hamiltonian in the ground and excited states and computing the sum of all transitions. A calculated splitting is predicted even for the case of an anisotropic interaction of the electronic magnetic moment with only one ligand nuclear moment. This splitting is found to increase as the interactions with the eight nearest-neighbor fluorine nuclei are sequentially added as a result of the fact that the superhyperfine levels tend to form into two groups, separated from one another energetically. The magnetic dipole-dipole interaction contributes about 70% of the observed splitting and with the inclusion of transferred spin and contact terms excellent agreement is obtained between the observed and calculated doublet structure of the line shape. In the general case, if the widths of the individual superhyperfine transitions are less than the energy of interaction between the paramagnetic ion and the nuclear magnetic moments of the ligand ions, a complicated structure of optical lines may be observed even in zero applied magnetic field. Then the number of components and their relative intensities will depend on the parameters of the transferred hyperfine interaction.

ACKNOWLEDGMENTS

We thank Dr. A. Cassanho for growing the sample which was also used in Ref. 1. The support of the National Science Foundation, Grant No. DMR-9321052, is gratefully acknowledged.

APPENDIX

Magnetic dipole-dipole coupling constants for Eqs. (3) and (4)

$$a_{xx,d}(i) = K_i g_\perp (\cos\varphi - 3x_i(x_i\cos\varphi + y_i\sin\varphi)/r_i^2),$$

$$a_{yy,d}(i) = K_i g_\perp (\cos\varphi - 3y_i(y_i\cos\varphi - x_i\sin\varphi)/r_i^2),$$

$$a_{xy,d}(i) = K_i g_\perp (-\sin\varphi - 3x_i(y_i\cos\varphi - x_i\sin\varphi)/r_i^2),$$

$$a_{yx,d}(i) = K_i g_\perp (\sin\varphi - 3y_i(x_i\cos\varphi + y_i\sin\varphi)/r_i^2),$$

$$a_{xz,d}(i) = -3K_i g_\parallel x_i z_i / r_i^2,$$

$$a_{yz,d}(i) = -3K_i g_\parallel y_i z_i / r_i^2,$$

$$a_{zz,d}(i) = K_i(1 - 3z_i^2/r_i^2) g_\parallel,$$

$$a_{zx,d}(i) = -3K_i g_\perp (x_i \cos\varphi + y_i \sin\varphi) z_i / r_i^2,$$

$$a_{zy,d}(i) = -3K_i g_\perp (y_i \cos\varphi - x_i \sin\varphi) z_i / r_i^2,$$

where $K_i = -\beta\gamma_F\hbar/r_i^3$; r_i is the radius vector of the ligand i, and the fluorine nuclear gyromagnetic ratio $\gamma_F/2\pi = 4007$ Hz/G.

Two examples of spin transfer and contact coupling constants for the $^4F_{3/2}(1)$ state

$$a_{zz,s}(i) = -A_{2s}\lambda_{2s}^2(7d_{03}^2 + 2d_{02}^2 + 7d_{01}^2 + 5d_{00}^2)/35; \tag{A1}$$

$$a_{zz,p}(i) = A_{2p}\{5[35(r_3^2 - t_3^2) + 30(r_2^2 - t_2^2) + 27(r_1^2 - t_1^2)] - 7(2s_3^2 - r_3^2 - t_3^2) - 2(2s_2^2 - r_2^2 - t_2^2) - 7(2s_1^2 - r_1^2 - t_1^2) - 10(s_0^2 - r_0^2)$$
$$- 3[2\sqrt{5}(r_2 s_1 - s_2 t_1) + \sqrt{6}(r_1 s_0 + s_1 r_0)]\}/35. \tag{A2}$$

Here $A_{2s} = (16\pi\beta\gamma_F\hbar/3)|\psi_{2s}(0)|^2 = 46$ GHz, $A_{2p} = (4\beta\gamma_F\hbar/5)\langle r^{-3}\rangle_{2p} = 2.52$ GHz,[20] and

$$d_{00} = 0.5\cos\theta(5\cos^2\theta - 3); \quad d_{01} = -0.25\sqrt{3}\sin\theta(5\cos^2\theta - 1);$$

$$d_{02} = 0.25\sqrt{30}\sin^2\theta\cos\theta; \quad d_{03} = -0.25\sqrt{5}5\sin^3\theta;$$

$$d_{11} = -(1+\cos\theta)(1 + 10\cos\theta - 15\cos^2\theta)/8; \quad d_{-11} = (1-\cos\theta)(-1 + 10\cos\theta + 15\cos^2\theta)/8;$$

$$d_{12} = -(10)^{1/2}\sin\theta(1+\cos\theta)(3\cos\theta - 1)/8; \quad d_{-12} = -(10)^{1/2}\sin\theta(1-\cos\theta)(3\cos\theta + 1)/8;$$

$$d_{13} = (15)^{1/2}\sin^2\theta(1+\cos\theta)/8; \quad d_{-13} = (15)^{1/2}\sin^2\theta(1-\cos\theta)/8;$$

$$s_0 = \lambda_{2\sigma} d_{00}\cos\theta + \sin\theta\lambda_{2\pi} d_{01}; \quad s_1 = \lambda_{2\sigma} d_{01}\cos\theta - 0.5\sin\theta\lambda_{2\pi}(d_{11} - d_{-11});$$

$$s_2 = \lambda_{2\sigma} d_{02}\cos\theta - 0.5\sin\theta\lambda_{2\pi}(d_{12} - d_{-12}); \quad s_3 = \lambda_{2\sigma} d_{03}\cos\theta - 0.5\sin\theta\lambda_{2\pi}(d_{13} - d_{-13});$$

$$r_0 = -\lambda_{2\sigma} d_{00}\sin\theta/\sqrt{2} + \cos\theta\lambda_{2\pi} d_{01},$$

$$r_1 = -\lambda_{2\sigma} d_{01}\sin\theta/\sqrt{2} - 0.5\lambda_{2\pi}[\cos\theta(d_{11} - d_{-11}) + (d_{11} + d_{-11})],$$

$$r_2 = -\lambda_{2\sigma} d_{02}\sin\theta/\sqrt{2} - 0.5\lambda_{2\pi}[\cos\theta(d_{12} - d_{-12}) + (d_{12} + d_{-12})],$$

$$r_3 = -\lambda_{2\sigma} d_{03}\sin\theta/\sqrt{2} - 0.5\lambda_{2\pi}[\cos\theta(d_{13} - d_{-13}) + (d_{13} + d_{-13})],$$

$$t_1 = \lambda_{2\sigma} d_{01}\sin\theta/\sqrt{2} + 0.5\lambda_{2\pi}[\cos\theta(d_{11} - d_{-11}) - (d_{11} + d_{-11})],$$

$$t_2 = \lambda_{2\sigma} d_{02}\sin\theta/\sqrt{2} + 0.5\lambda_{2\pi}[\cos\theta(d_{12} - d_{-12}) - (d_{12} + d_{-12})],$$

$$t_3 = \lambda_{2\sigma} d_{03}\sin\theta/\sqrt{2} + 0.5\lambda_{2\pi}[\cos\theta(d_{13} - d_{-13}) - (d_{13} + d_{-13})].$$

[1] R. M. Macfarlane, R. S. Meltzer, and A. Cassanho, Phys. Rev. Lett. **69**, 542 (1992).

[2] P. F. A. Klinkenberg, Physica (Amsterdam) **11**, 327 (1945); Yu. P. Dontsov, V. A. Morosov, and A. R. Striganov, Opt. Spectrosc. **8**, 391 (1960); S. Gerstenkorn and J.-M. Helbert, C. R. Seances Acad. Sci., Ser. B **266**, 546 (1968); W. H. King, A. Stoudel, and M. Wilson, Z. Phys. **265**, 207 (1973); K. A. H. van Leeuwen, E. R. Eliel, B. H. Post, and W. Hogervorst, Z. Phys. A **301**, 95 (1981); Lu Fuquan *et al.*, Phys. Rev. A **44**, 1843 (1991).

[3] B. Z. Malkin and S. K. Saikin, Proc. SPIE **2706**, 193 (1996).

[4] G. F. Imbusch, W. M. Yen, A. L. Schawlow, G. E. Devlin, and J. P. Remeika, Phys. Rev. **136**, A481 (1964).

[5] N. Pelletier-Allard and R. Pelletier, J. Phys. C **17**, 2129 (1984).

[6] U. Ranon and J. S. Hyde, Phys. Rev. **141**, 259 (1966).

[7] J. M. Baker and J. P. Hurrell, Proc. Phys. Soc. London **82**, 742 (1963).

[8] R. G. Bessent and W. Hayes, Proc. R. Soc. London, Ser. A **285**, 430 (1965).

[9] N. I. Agladze, M. N. Popova, G. N. Zhizhin, V. J. Egorov, and M. A. Petrova, Phys. Rev. Lett. **66**, 477 (1991).

[10] N. Karayianis, J. Phys. Chem. Solids **32**, 2385 (1971).

[11] J. P. Sattler and J. Nemarich, Phys. Rev. B **4**, 1 (1971).

[12] N. Bloembergen, Physica (Amsterdam) **15**, 386 (1949); R. M. Shelby, C. S. Yannoni, and R. M. Macfarlane, Phys. Rev. Lett. **41**, 1739 (1978); A. Szabo, T. Muramoto, and R. Kaarli, Phys. Rev. B **42**, 7769 (1990).

[13] J. Ganem, Y. P. Wang, D. Boye, R. S. Meltzer, W. M. Yen, and R. M. Macfarlane, Phys. Rev. Lett. **66**, 695 (1991).

[14] Y. P. Wang, D. P. Landau, R. S. Meltzer, and R. M. Macfarlane, J. Opt. Soc. Am. B **9**, 946 (1992).
[15] P. Blanchfield and G. A. Saunders, J. Phys. C **12**, 4673 (1979).
[16] A. da Gama, G. F. de Sa, P. Porcher, and P. Caro, J. Chem. Phys. **75**, 2583 (1981).
[17] L. A. Bumagina, V. I. Krotov, B. Z. Malkin, and A. Kh. Khasanov, Sov. Phys. JETP **53**, 792 (1981).
[18] H. De Leebeeck and C. Gorller-Walrand, J. Alloys Compd. **225**, 75 (1995).
[19] M. A. Couto dos Santos, P. Porcher, J. C. Krupa, and J. A. Geslaud, J. Phys.: Condens. Matter **8**, 4643 (1996).
[20] B. R. McGarvey, J. Chem. Phys. **65**, 955 (1976).
[21] M. Wolfsberg and L. Helmholz, J. Chem. Phys. **20**, 837 (1952).
[22] D. Garcia and M. Faucher, J. Chem. Phys. **82**, 5554 (1985).